COMPUTER METHODS IN MATERIALS SCIENCE

2025, vol. 25, no. 2, 17–25
https://doi.org/10.7494/cmms.2025.2.1019

Evaluation of deformation inhomogeneity in multi-layered steel-titanium and steel-magnesium systems

Bartłomiej Pabich*, Bartłomiej Żurowski, Marcin Kwiecień, Janusz Majta

AGH University of Krakow, A. Mickiewicza 30 av., 30-059 Krakow, Poland.

Abstract

In the presented study, plastometric tests using channel die compression were employed to define the boundary conditions for numerical simulations of the deformation processes of heterogeneous multi-layer systems composed of microalloyed steel, titanium, or magnesium. Various configurations, conditions, and deformation schemes were applied, which were then replicated in numerical simulations. Rheological models were used in the studies which, through computer simulations, enabled the modeling of interactions between the incoherent components of the microstructure. The primary outcome of the conducted experimental studies and numerical simulations is the ability to assess the heterogeneity of the studied multi-layer systems in terms of their mechanical states and influence on microstructural changes. This heterogeneity additionally arises from the diverse microstructural and rheological characteristics of the investigated materials (BCC vs. HCP), which, in turn, affect the strengthening mechanisms, primarily strain hardening. The results obtained from channel die compression tests were then used in simulations of multi-stage wire drawing, supporting both the design phase and the analysis of the resulting microstructural effects in the studied heterogeneous systems. It was observed that one of the key criteria for designing heterostructured wires from the examined materials is the proper selection of the volume fraction of the components, as well as the deformation history during multi-stage wire drawing, considering interpass heat treatment.

Keywords: heterostructured materials, multi-layered composite, multi-stage wire drawing, numerical simulation

1. Introduction

It is well known that combining two metallic materials with significantly different plasticity in a multi-layer system – due to differences in their crystal lattice, the number of possible slip systems, stacking fault energy (SFE), chemical composition, phase composition, morphology, and the degree of microstructure refinement – can result in an attractive combination of mechanical properties (Wu & Zhu, 2017). Similar advantages can also be found in other material systems (That, 2024).

In the presented research, the investigated material consisted of a microalloyed steel matrix, characterized by high strength and good ductility during plastic deformation (Majta et al., 2017), along with titanium or magnesium layers exhibiting limited plasticity. The choice of the above materials was supported by the literature focusing on combining materials such as Fe-Cu, Fe-Al, or Ti and Cu, using roll forming to obtain a layered composite with complex morphology and microstructure development (McCabe et al., 2021; Yu et al., 2014). The main advantage of a material with such an inhomogeneous structure is the synergistic effect of the HCP phase existing as thin layers within the ductile BCC-phase matrix – i.e., microalloyed steel strengthened by precipitation and ferrite grain refinement. Effective control of such inhomogeneities is essential, as their evolution can have both negative and positive outcomes. On the

* Corresponding author: bpabich@agh.edu.pl
ORCID ID's: 0009-0002-0379-4195 (B. Pabich), 0000-0002-2938-4672 (M. Kwiecień), 0000-0001-8603-6677 (J. Majta)

one hand, excessive nonuniformity may lead to premature failure or uncontrolled fragmentation of reinforcing layers; on the other, a controlled transition from a strictly layered arrangement to a composite structure with dispersed reinforcement can enhance and combine the properties of individual composite components (Hoagland et al., 2002; Koseki et al., 2014).

2. Experimental

Channel die compression tests were performed on the multi-layer samples to experimentally determine their mechanical state, i.e., the distributions of strain and stress during deformation. The tests aimed to replicate the conditions that the materials experience during metal forming operations. The samples had a length of 15 mm and a width of 10 mm and consisted of microalloyed steel layers with thicknesses of 2 mm or 4 mm and an inner titanium/magnesium layer of 1 mm thickness. Each sheet surface was prepared by degreasing and grinding with 500 grit sandpaper, no lubrication was used during process. Such packages underwent deformation with strain magnitudes of 0.25 and 0.5. The schematic and example of deformed samples are presented in Figure 1 and the characteristics of the research materials used are in Table 1.

The channel die compression tests and the performed analysis of their results allowed for the characterization of the complex rheological properties and the evolution of the microstructure in the studied multi-layer systems. It was demonstrated that differences in the thickness of the matrix material significantly affect the plastic flow behavior, ultimately leading to an inhomogeneous distribution of work hardening among the individual layers (Pabich et al., 2024). Additionally, a multi-stage wire drawing process of heterostructured, multi-layered materials was performed.

Table 1. Characteristics of research materials

	Microalloyed steel	Ti, grade 2	Mg, AZ31
Crystal structure	BCC	HCP	HCP
Shear modulus (*G*) [GPa]	78	43	17
Yield strength (*YS*) [MPa]	430	230	146
Tensile strength (*TS*) [MPa]	720	437	315
Elongation (*El*) [%]	14.8	47.0	20.2
Average hardness [HV0.1]	214	125	96
Chemical composition [wt%]	C: 0.07 Si: 0.29 Mn: 1.36 Nb: 0.067 Ti: 0.03 Cu: 0.16 N: 0.009 Fe: bal.	Fe: 0.01 H: 0.03 O: 0.04 N: 0.01 Ti: bal.	Al: 3.27 Zn: 0.98 Mn: 0.28 Fe: 0.0027 Ni: 0.00078 Cu: 0.0005 Si: 0.11 Mg: bal.
Initial grain size [μm]	22	28	20–25

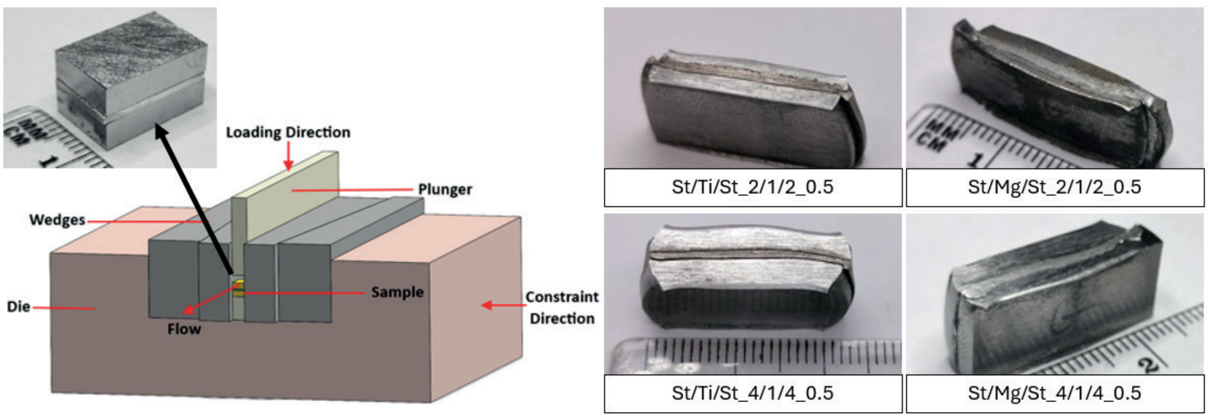

Fig. 1. Schematic and example of deformed multi-layered systems produced through channel die compression test

The investigated heterostructured system, subjected to deep wire drawing, consisted of a hollow microalloyed steel cylinder with a diameter of 6.5 mm and a rod of Ti or Mg with a diameter of 3.0 mm placed inside it, later referred to as TR (Tube/Rod) samples. The process involved reducing the wire diameter from 6.5 mm to 4.0 mm in 10 passes, with an effective strain per pass of approximately 0.10 and monosodium soap powder as a lubricant. Examination of the longitudinal section of the specimens at the 4.0 mm diameter showed cracks in the Mg layer, which eliminated this material as suitable for further drawing tests due to its inability to accumulate severe plastic deformation (Pabich et al., 2024). The initial material and schematic of the wire drawing process are presented in Figure 2. Vickers hardness tests (applied load 100 g, dwell time 10 s) and electron back-scattered diffraction (EBSD) analysis carried out on the 4.0 mm diameter wire (Fig. 3) showed that the steel exhibits greater strain hardening and grain refinement than the Ti layer, suggesting that the steel carries more strain in the initial stages of wire drawing.

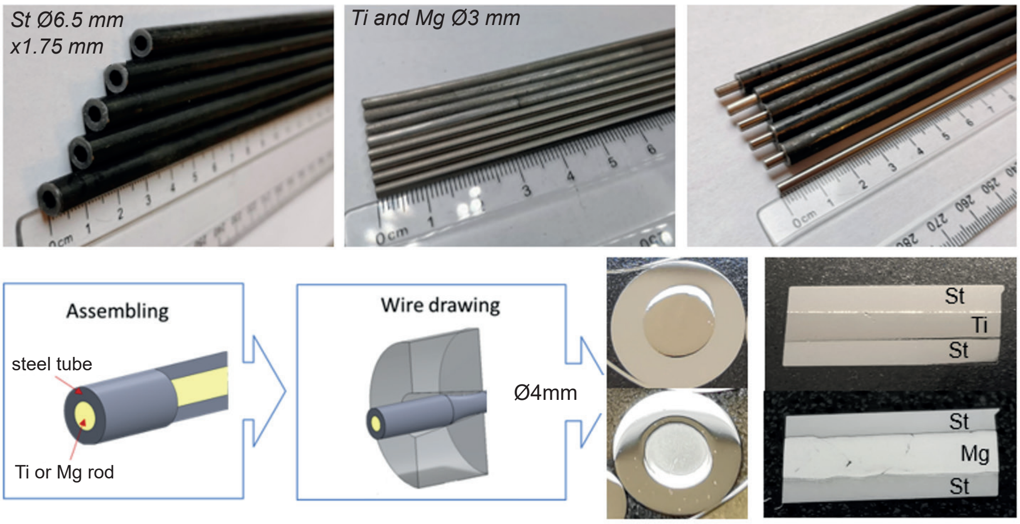

Fig. 2. A schematic representation with samples dimensions and process parameters of experimental studies

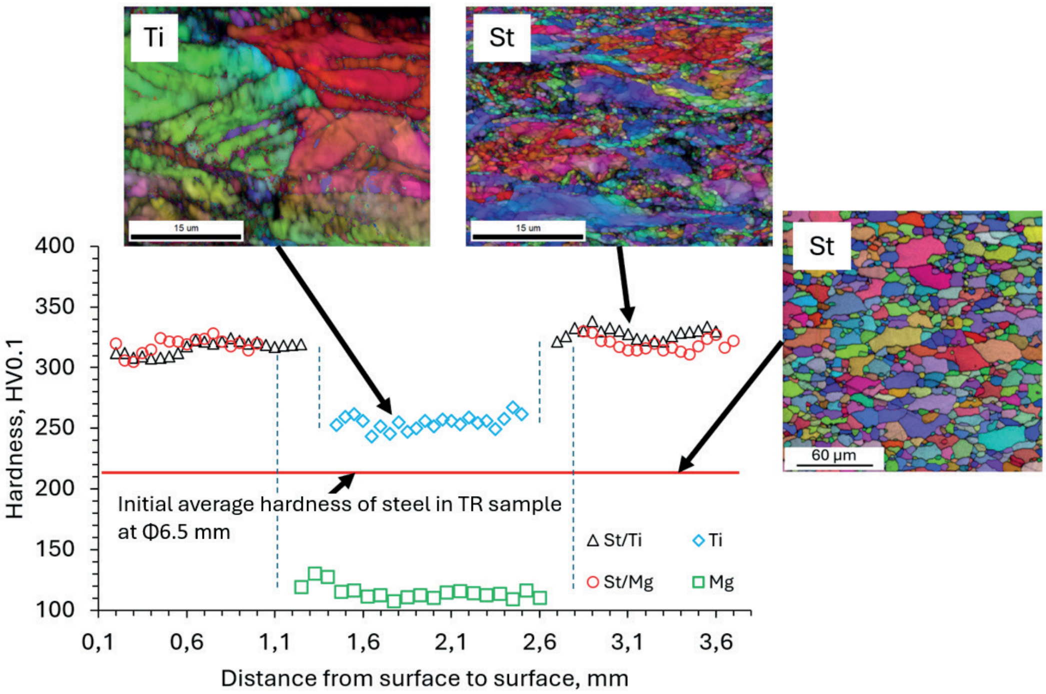

Fig. 3. Hardness test results and EBSD maps performed for TR samples at a diameter of 4 mm

3. Rheological models

The material data used in the computer-aided design (Yanagimoto et al., 2022) were selected from a database of commercial FEM software, Forge NxT, and from the literature (Majta, 2019). The data from the database was additionally compared with the results of plastometric tests carried out for initial materials. Based on the obtained stress-strain curves (Fig. 4), calculations were made and adjusted for the Hansel–Spittel equation (Chadha et al., 2018):

$$\sigma_f = A\exp(m_1 T)\varepsilon^{m_3}\dot{\varepsilon}^{m_3}\exp\left(\frac{m_4}{\varepsilon}\right)(1+\varepsilon)^{m_5 T}\cdot \exp(m_6 - \varepsilon)\dot{\varepsilon}^{m_7 T}T^{m_3} \quad (1)$$

where: σ_f – flow stress, A – material constant, ε – equivalent strain, $\dot{\varepsilon}$ – equivalent strain rate, T – deformation temperature, m_1–m_8 – constants defining the material's sensitivity to temperature, strain and strain rate.

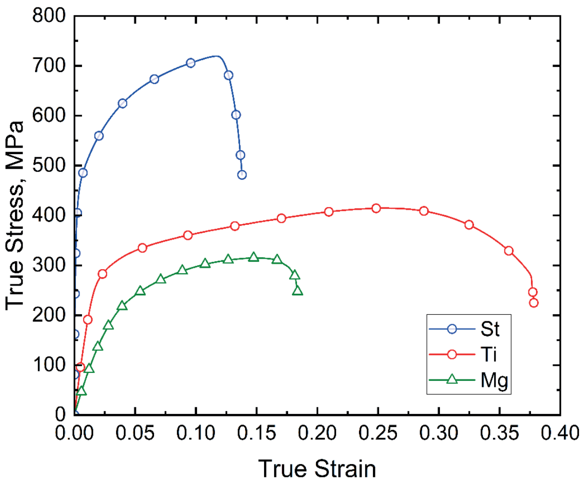

Fig. 4. Stress-strain curves obtained for initial materials

The resulting rheological data, together with material parameters, were implemented to simulate the deformation of multi-layer materials. Other material data, including thermal model coefficients, are presented in Table 2.

Table 2. Thermal coefficients of analyzed materials

Material	Specific heat capacity [J/(kg·K)]	Density [kg/m^3]	Thermal conductivity [W/(m·K)]	Emissivity
St	778	7,850	35.5	0.88
Ti	420	4,540	6.0	0.88
Mg	101	1,780	12.0	0.08

4. Numerical simulations

In the first part of the numerical simulations, a channel die compression test was reproduced using the Forge NxT software. The software allowed for assigning multiple materials to a single object sample when defining the spatial parameters, which resulted in significantly reduced computation time while maintaining correct results. To better understand the interaction between the layers, the simulations were modified by introducing different friction conditions, an additional layer of St and Ti or Mg, and by swapping the positions of the St layers with the Ti or Mg layers (Fig. 5a), as well as modifications in friction conditions, categorized as high, medium, and low/sliding friction, values of which are shown in Table 3. The influence of the friction coefficient on the deformation of layers is presented in Figure 5b. As a result, 12 variants with different layer configurations were obtained, from which data on temperature, stress, strain and material distributions were extracted.

Table 3. Values of used Coulomb friction coefficients

Coefficient	Friction conditions		
	low	medium	high
Static friction	0.00	0.10	0.40
Kinetic friction	0.00	0.05	0.20

The second numerical simulation developed was a representation of the multi-stage wire drawing process of the investigated multi-layered systems. The model represents the drawing process of a sample composed of two or three layers, successively representing two systems: Tube/Rod (TR) and Tube/Tube/Rod (TTR). In these systems, the outer layer always consisted of St, the inner rod consisted of Ti or Mg in the case of the TR system, and the inner tube was made of Ti/Mg and St rod in the case of the TTR system. The dimensions of the samples were 30 mm in length and 6.5 mm in diameter. The wire drawing process consisted of 7 passes, reducing the diameter of the wires from 6.5 mm to 5.2 mm. The diameters of the individual dies and the effective strain per pass are presented in Table 4.

Table 4. Diameters and strain obtained in individual passes of wire drawing

No. of pass	Diameter of the die (D_f) [mm]	Effective strain/pass, $\varepsilon = 2\ln(D_0/D_f)$
1	6.5	–
2	6.2	0.09
3	6.0	0.07
4	5.9	0.03
5	5.6	0.10
6	5.4	0.07
7	5.2	0.08

a)

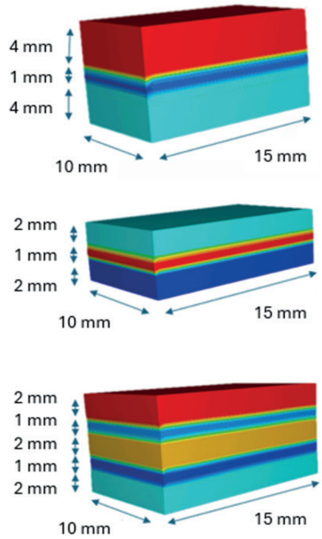

Material Layers	Layer Height, mm
St/Ti/St	4/1/4
St/Ti/St	2/1/2
Ti/St/Ti	4/1/4
Ti/St/Ti	2/1/2
St/Mg/St	4/1/4
St/Mg/St	2/1/2
Mg/St/Mg	4/1/4
Mg/St/Mg	2/1/2
St/Ti/St/Ti/St	2/1/2/1/2
Ti/St/Ti/St/Ti	2/1/2/1/2
St/Mg/St/Mg/St	2/1/2/1/2
Mg/St/Mg/St/Mg	2/1/2/1/2

b)

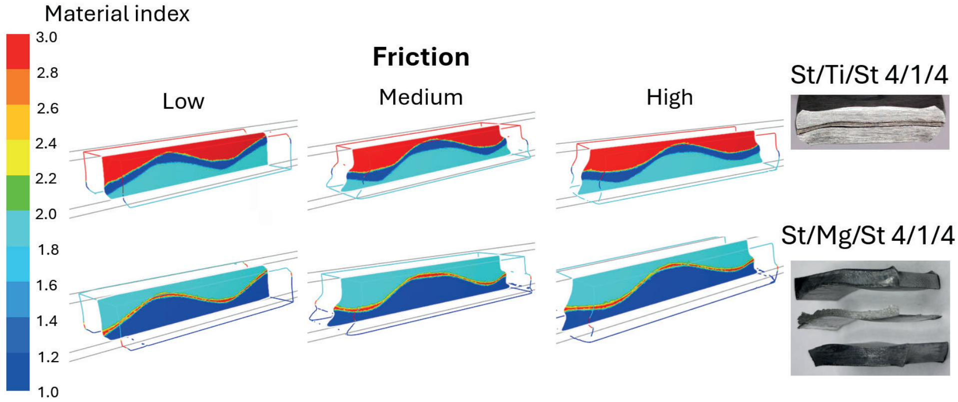

Fig. 5. Dimensions and layer configurations of defined samples for numerical calculations (a) and results of sample deformation under different friction coefficients (b)

As in the channel compression test, the individual material layers were assigned to a single object, the dimensions of which are presented in Figure 6. In the case of friction parameters, the analysis of friction-free conditions was abandoned as purely theoretical. The results of the obtained simulations were extracted similarly to the channel test. During the simulations, a fully coupled thermo-mechanical model was used with tetragonal finite elements. The mesh size was selected based on the initial trials to provide acceptable simulation time and accuracy. Depending on the number of layers, the number of finite elements varied between approximately 100,000 and 160,000. In order to avoid numerical errors related to interpolation along the material contact surface, remeshing was not used during the analysis.

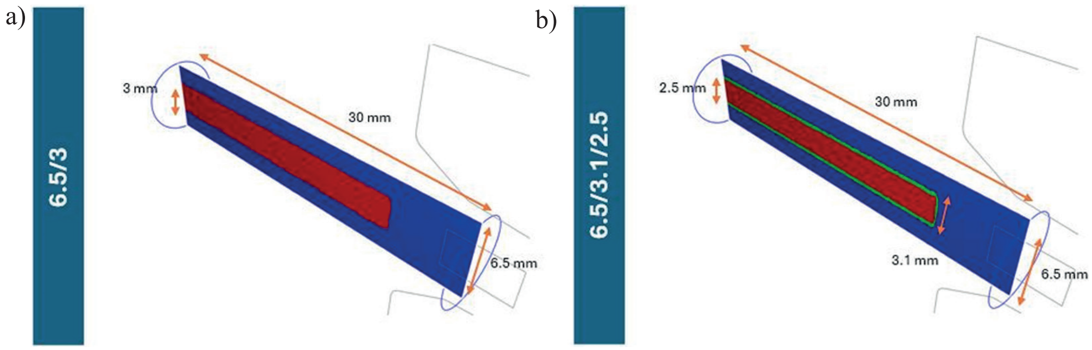

Fig. 6. Initial dimensions of TR (a) and TTR sample (b)

5. Results

Complex simulations of the channel compression tests, with multiple configurations of materials, layers and friction coefficients, have provided a better understanding of the deformation behavior of multi-layer systems. A comparison of the simulation results with the dimensions and geometry of the deformed specimens showed that the best correlating results are those obtained with the medium value of the friction coefficient. Depending on the chosen configuration, the system either deformed relatively uniformly without any pronounced serpentining or thinning of the inner layers, as in the case of 4/1/4, 2/1/2 – Mg/St/Mg and Ti/St/Ti (Fig. 7a) as well as 2/1/2/1/2 – Mg/St/Mg/St/Mg and Ti/St/Ti/St/Ti. However, it can be observed that there is pinching in the steel at the center of the layer. In the case of specimens with magnesium or titanium as the inner material, in the 4/1/4, 2/1/2 St/Ti/St and St/Mg/St and 2/1/2/1/2 St/Ti/St/Ti/St and St/Mg/St/Mg/St systems very intense wave formation and thinning occur in the middle layers, which would be beneficial for their fracture and particle formation (Fig. 7b).

The analysis of the results shows a correlation between temperature and strain. As expected, higher temperature values are observed in areas with higher deformation. Likewise, a similarity can be seen in the field pattern of these two parameters (Fig. 8a). The highest temperature occurs at the central point of the samples. In all cases, higher values of Von Mises Equivalent Stress can be observed in St layers compared to Ti or Mg. It is also worth noting that in the case of samples where wave formation occurs in the inner layers, the stress present in the material above the peak of the waves is lower than that "below" them (Fig. 8b). This leads to inhomogeneities in strain hardening not only at the cross-section of the material layers but also at the matrix layers of material. Both wave formation in inner layer of samples and stress variations within steel layers are direct consequences of the upsetting process which is characterized by x-shaped distribution of stress, rheological differences between the constituent materials and stress-induced fluctuations at the contact surface of layers. The shape of the produced wave is a function of shear modulus and the ratio of the thickness of the layers used (Junqua & Grilhé, 1995).

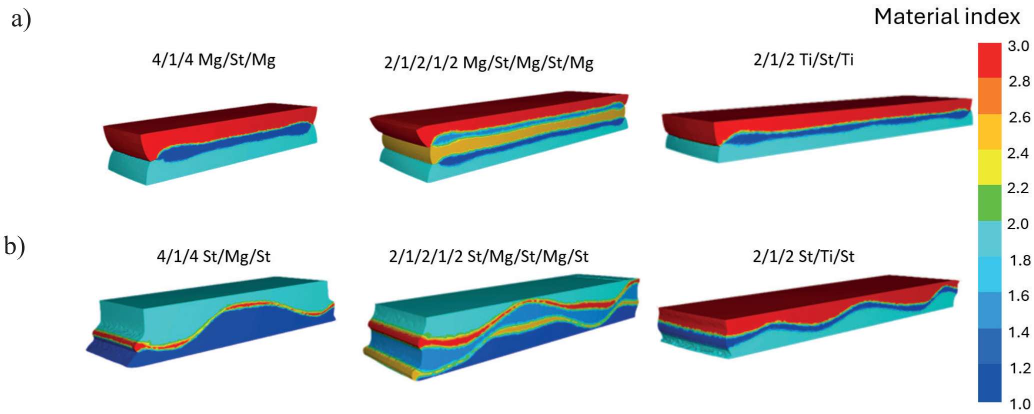

Fig. 7. Selected deformed layer configurations characterized by: a) uniform deformation; b) wave formation of inner layers

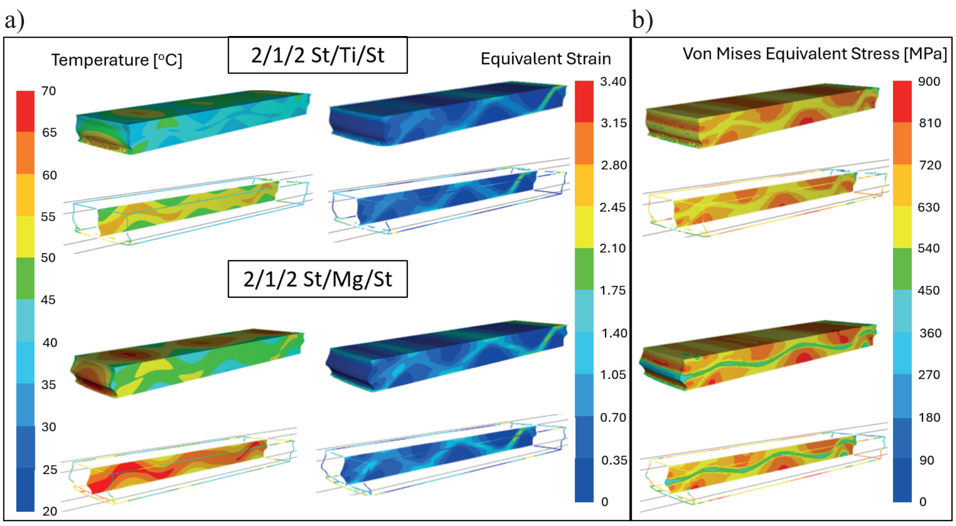

Fig. 8. Temperature, strain (a) and stress (b) distribution for selected St/Ti and St/Mg systems

Based on the results of the channel compression test, the second part of the simulation of the drawing process of the heterogeneous system was carried out. As a result of the results obtained from the first part, the construction of a multi-layer inhomogeneous system was proposed, i.e. TTR and TR in both systems the composite materials were microalloyed steel as the matrix and Ti or Mg in the TTR system a tube and in TR system a rod.

As demonstrated by the channel compression tests, the deformation conditions and process parameters – i.e., the size and number of drafts for specific layer thicknesses of the systems – are crucial in the development of both the rheology and the microstructure of the constituent materials. For this reason, it was necessary to prepare simulations of the investigated TTR and TR systems during the production process of multi-layered wires, taking into account the characteristics of the drawing process. This process differs significantly from other plastic forming methods due to the shape of the tool (tapered die) and the nature of material flow through the tool. A direct consequence is the high inhomogeneity in the cross-section of the drawn products. Moreover, the heterogeneous system – comprising different materials with varying rheological characteristics – results in a drawing process outcome that varies significantly for the final products.

The boundary conditions for the simulation process were designed, as presented in the experimental section, and it was demonstrated that the ability to visualize the mechanical state in drawn heterogeneous systems constitutes a very significant indicator for the strengthening processes of these materials. In other words, the superposition of the mechanical state – characterized by the inhomogeneity of strains and stresses in the examined systems – and the associated strengthening processes, both deformation-induced and microstructural, resulted in different behaviors among the studied systems.

The numerical simulations were conducted to analyze the processes of deformation and work hardening during the multi-stage wire drawing process of two configurations of heterogeneous systems: Tube/Rod (St/Ti) and Tube/Tube/Rod (St/Ti/St) (Fig. 9). As demonstrated during the drawing process, there is a significant difference in the distribution of stresses in the material. In the case of the TR system, higher stress values are found in the near-surface layers – the steel – of the deformed wires, while in the case of TTR, the interaction field is larger and reaches higher values in the layer of the inner rod. These differences are all the more apparent in the initial passes of the drawing process (Fig. 10). In the initial passes, it is apparent that the steel as a matrix carries higher stresses in both TR and TTR, particularly at layers close to the wire surface. In addition, a comparison of Ti to Mg also shows that the stress values in the Mg layer are lower than those in the Ti layers.

The effect of the friction coefficient on temperature and strain is shown in Figure 11, a higher value of the coefficient leads to an increase in the obtained temperatures at the cross-section of the specimen from 36°C to 42°C. In the case of deformation, the values obtained are not significantly affected, but it is noticeable that the Ti or Mg layer is more displaced at the beginning of the sample.

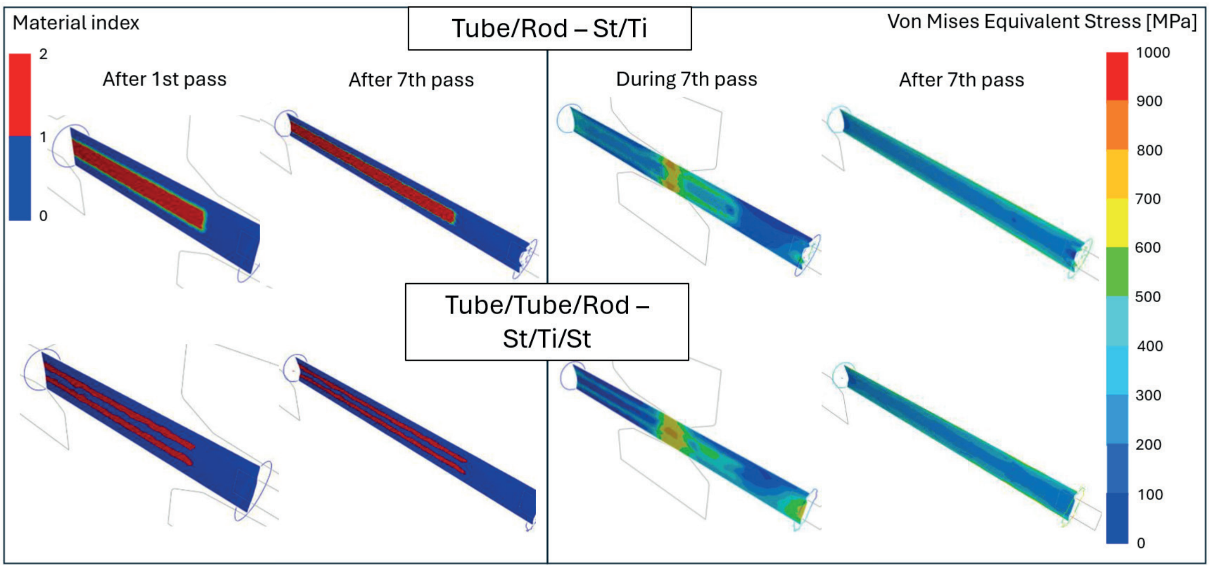

Fig. 9. Selected simulation results for Ti, TR and TTR specimens: representation of material distribution after the 1st and 7th pass, and stresses during and accumulated at the 7th pass

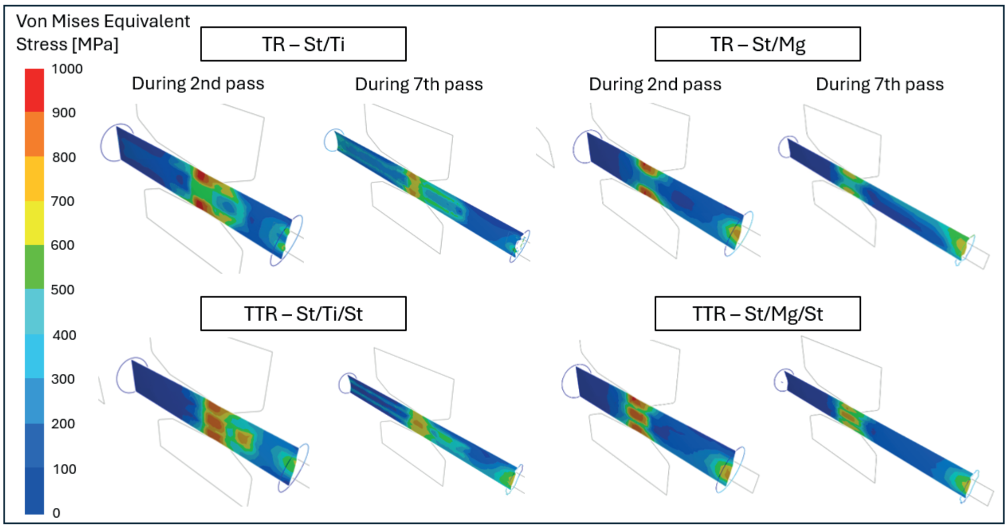

Fig. 10. Comparison of von Mises equivalent stress at the longitudinal section of each system during the 2nd and 7th pass

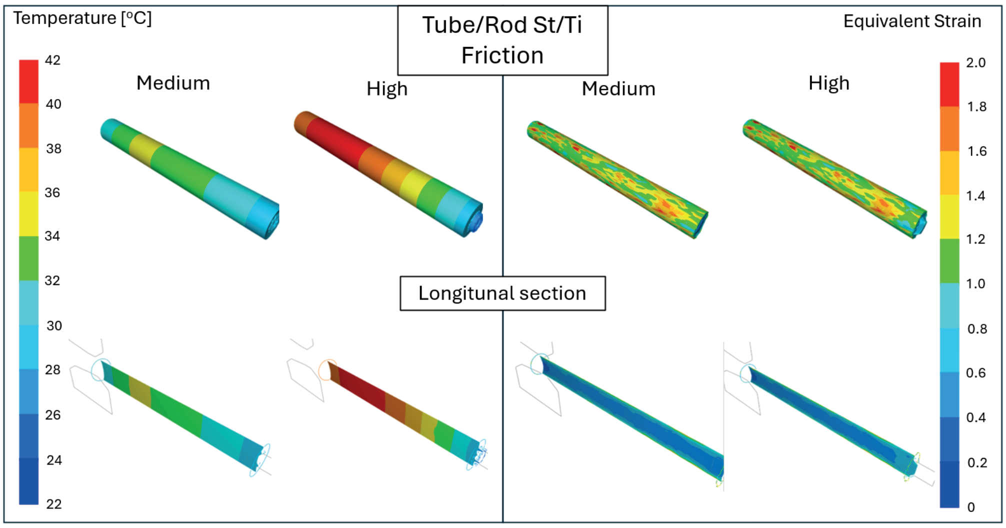

Fig. 11. Influence of friction value on values of temperature and equivalent strain on the example of TR St/Ti sample

Based on the data gathered from initial experiments and numerical simulations, a methodology was developed to evaluate the influence of wire drawing process parameters on the fragmentation of titanium layers, which are less ductile than the steel matrix. This led to the production of Tube/Rod and Tube/Tube/Rod wires with a diameter of ⌀0.3 mm, the microstructures of which are shown in Figure 12.

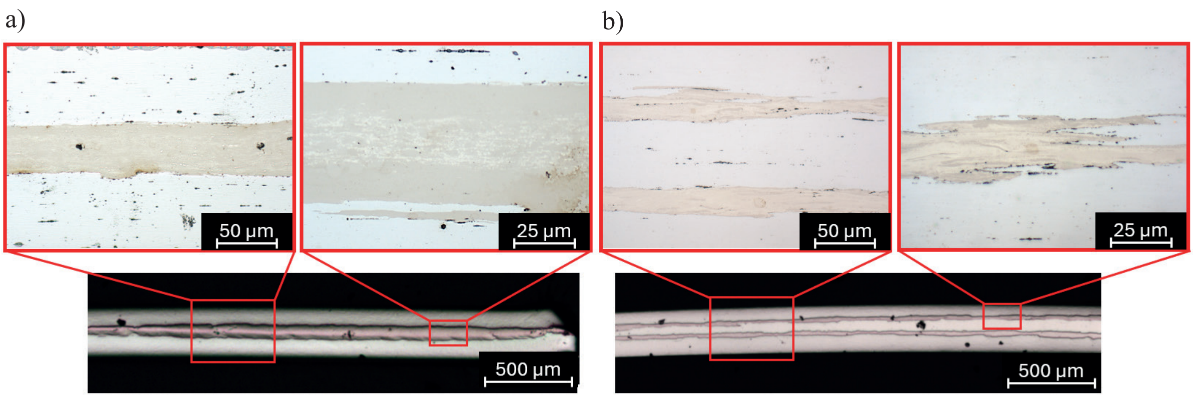

Fig. 12. Microstructures from the longitudinal section of ⌀0.3 mm wires: a) Tube/Rod; b) Tube/Tube/Rod

6. Summary and conclusions

The presented research focused on computer-aided analysis of the wire manufacturing process, characterized not only by mechanical inhomogeneity but also by a material structure consisting of a continuous matrix, i.e., relatively ductile microalloyed steel, in which Ti particles of various sizes are present. These particles were formed as a result of titanium fragmentation following intense deformation of the inhomogeneous steel/Ti system. The obtained results allow the formulation of the following conclusions:

- The results obtained from channel die compression tests – both numerical simulations and experimental studies – were used in the simulations of multi-stage wire drawing. These results supported both the design phase and the analysis of the resulting microstructural effects in the studied heterogeneous systems. The numerical simulations proved to be a valuable tool for understanding plastic deformation processes in heterogeneous systems, particularly during multi-stage wire drawing operations involving a high accumulation of deformation energy.
- The stress and strain field calculations facilitated the analysis of the resulting microstructures, which directly reflect the applied process parameters, inter-operational heat treatment conditions, and the diverse material properties of the materials used.
- The observed heterogeneity in stress and strain fields arises from the differing microstructural and rheological properties of the studied materials (body-centered cubic – BCC vs. hexagonal close-packed – HCP structures). These differences significantly influence the strengthening mechanisms, particularly work hardening.
- One of the key criteria in designing heterostructured wires from the studied materials is the appropriate selection of the volume fraction of the components and the deformation history during multi-stage wire drawing, including inter-operational heat treatment. It should be emphasized that a critical factor in this context is the variation in rheological properties among the components of the examined multilayered systems.

Acknowledgements

The research was funded entirely by National Science Centre, Poland, grant number: OPUS 2022/45/B/ST8/01383.

References

Chadha, K., Shahriari, D., & Jahazi, M. (2018). An approach to develop Hansel–Spittel constitutive equation during ingot breakdown operation of low alloy steels. In M. Muruganant, A. Chirazi, B. Raj (Eds.), *Frontiers in Materials Processing, Applications, Research and Technology. Select Proceedings of FiMPART 2015* (pp. 239–246). Springer Singapore. https://doi.org/10.1007/978-981-10-4819-7_20

Hoagland, R. G., Mitchell, T. E., Hirth, J. P., & Kung, H. (2002). On the strengthening effects of interfaces in multilayer fee metallic composites. *Philosophical Magazine A*, *82*(4), 643–664. https://doi.org/10.1080/01418610208243194

Junqua, N., & Grilhé, J. (1995). Interface instabilities of multilayers and flat precipitates. *Philosophical Magazine A*, *71*(5), 1125–1134. https://doi.org/10.1080/01418619508236240

Koseki, T., Inoue, J., & Nambu, S. (2014). Development of multilayer steels for improved combinations of high strength and high ductility. *Materials Transactions*, *55*(2), 227–237. https://doi.org/10.2320/matertrans.M2013382

Majta, J. (2019). *Odkształcanie i własności metali. Stale mikrostopowe. Wybrane zagadnienia* [Deformation and Properties of Metals. Microalloyed Steels. Selected Problems] (wyd. 2). Wydawnictwa AGH.

Majta J., Kwiecień M., Lisiecka-Graca P., Błoniarz R., Kopytek E., & Muszka K. (2017). Precipitation-based strengthening mechanisms in ultrafine-grained and nano-structures in microalloyed steel wires. *11th International Conference on Advanced Computational Engineering and Experimenting ACE-X* [unpublished].

McCabe, R. J., Nizolek, T. J., Li, N., Zhang, Y., Coughlin, D. R., Miller, C., & Carpenter, J. S. (2021). Evolution of microstructures and properties leading to layer instabilities during accumulative roll bonding of Fe–Cu, Fe–Ag, and Fe–Al. *Materials & Design*, *212*, 110204. https://doi.org/10.1016/j.matdes.2021.110204

That, L. H. T. (2024). Functionally graded porous material and its application in sandwich beams for bending and vibration behaviors. *Computer Methods in Materials Science*, *24*(1), 15–24. https://doi.org/10.7494/cmms.2024.1.0832

Wu, X., & Zhu, Y. (2017). Heterogeneous materials: a new class of materials with unprecedented mechanical properties. *Materials Research Letters*, *5*(8), 527–532. https://doi.org/10.1080/21663831.2017.1343208

Yanagimoto, J., Banabic, D., Banu, M., & Madej, L. (2022). Simulation of metal forming – Visualization of invisible phenomena in the digital era. *CIRP Annals*, *71*(2), 599–622. https://doi.org/10.1016/j.cirp.2022.05.007

Yu, H., Tieu, A. K., Lu, Ch., Liu, X., Godbole, A., Li, H., Kong, Ch., & Qin, Q. (2014). A deformation mechanism of hard metal surrounded by soft metal during roll forming. *Scientific Reports*, *4*(1), 5017. https://doi.org/10.1038/srep05017